Developments in the use of ultra high performance fiber reinforced concrete as strengthening material

Developments in the use of Ultra High Performance Fiber Reinforced Concrete as Strengthening Material

Dr Spyridon Paschalis[a*], Dr Andreas Lampropoulos[b]

[a] School of Engineering, Department of Civil Engineering, University of Bolton, UK

[b] School of Environment and Technology, University of Brighton, UK

Abstract

Ultra High Performance Fiber Reinforced Concrete (UHPFRC) is a novel material which has been developed the last few decades and has been applied in applications that require high strength, ductility and durability. Recently, the material has been applied in strengthening applications. The present study aims to investigate new techniques for the application of UHPFRC as strengthening material and to provide an insight into the parameters affecting the performance of elements strengthened with UHPFRC. The present research investigates for the first time the effectiveness of the use of dowels at the interface between UHPFRC and concrete, to improve the connection between these two materials. Additionally, the effectiveness of the use of UHPFRC jackets for the strengthening of Reinforced Concrete (RC) beams has been examined. In the present research, a systematic experimental study has been conducted together with numerical study.

The results demonstrate that both examined techniques are effective and should be taken into consideration when UHPFRC is applied for strengthening material. The dowels result in better bonding at the interface and can delay the formation of cracks in the post elastic phase, leading to reduced interface slip values and subsequent enhanced load bearing capacity. This technique should be taken into consideration to eliminate the risk of premature de-bonding of the strengthening layer. The construction of UHPFRC jackets on the other hand, results in a

dramatic increase of the stiffness and the load carrying capacity of the strengthened elements and should be preferred in cases of heavily damaged RC members.

Keywords

Strengthening; Ultra High Performance Concrete; Full scale; Beams; UHPFRC jackets

1. Introduction

The structural upgrade of existing structures is a key priority worldwide. Nowadays, there are many available strengthening techniques. However, the extensive preventative application of these techniques for the protection of existing structures cannot be applied mostly due to issues linked to difficulties during the application of the techniques, which require special expertise, increased cost and construction time.

The present research focus on the application of an advanced material, such as the Ultra High Performance Fiber Reinforced Concrete (UHPFRC), for the strengthening of Reinforced Concrete (RC) members. The examined technique present crucial advantages which are related to the enhanced properties of the material and durability, and ease of preparation and application of the material. Another advantage of the examined technique is that thin elements with high strength and ductility can be constructed and therefore the dimensions of the strengthened elements do not change dramatically.

There are numerous published studies on the development and characterisation of the mechanical properties of UHPFRC [1-7]. The fiber distribution is an important parameter affecting the performance of UHPFRC and this was thoroughly investigated by Ferrara et al. [1]. Nicolaides et al. [2], developed an optimum mixture of Ultra High Performance Cementitious Composite with materials which were locally available in Cyprus, while Paschalis and Lampropoulos [3], investigated the effect of fiber content and curing time regimes on the tensile characteristics of UHPFRC. In this study it was found that the fiber

content significantly affects the tensile characteristics of UHPFRC, and different stress-strain models for various typical fibers contents, were proposed. The mechanical characteristics of UHPFRC under different loading conditions, including static and cyclic loading, have been studied in previously published studies [4-7].

The application of UHPFRC for the retrofitting of existing RC members has also been studied recently [8-12]. Bruhwiler and Denarie [8], applied UHPFRC in a series of rehabilitation applications, such as in a road bridge, a bridge pier and an industrial floor. Al-Osta et al. [9], studied the effectiveness of different techniques for the strengthening of RC beams using prefabricated UHPFRC strips and comparisons were made with cast-in-situ UHPFRC layers. Different strengthening configurations, such as strengthening on different sides of the beams were also investigated in this study. Safdar et al. [10], applied UHPFRC as a repair material and found that this application can increase mainly the stiffness of the strengthened elements. Lampropoulos et al. [11], presented a numerical investigation on the performance of UHPFRC for the flexural strengthening of RC beams and the effectiveness of the technique was highlighted. Paschalis et al. [12], presented an experimental and numerical investigation on the performance of UHPFRC for the flexural strengthening of full scale RC beams. In this study, UHPFRC layers with and without the use of steel bars in the layers were used for the strengthening of RC beams, and it was found that the UHPFRC layers can increase the stiffness of the strengthened members, while the addition of steel bars to the layers can produce a big increase of the load carrying capacity. Finally, a better bonding between UHPFRC and concrete was identified compared to concrete to concrete interfaces. However, in this study it was found that the slips at the interface were not negligible. On the contrary, high values of slip at the interface were recorded in the post-elastic region.

Based on existing studies, the application of UHPFRC can be effectively used to enhance the stiffness of the strengthened elements, while the load bearing capacity can also be

further increased with the addition of steel bars. However, the addition of steel bars is a labour-intensive technique and requires a minimum thickness for the strengthening layer leading to significant changes in the geometry and the characteristics of the initial structure.

The present study aims to investigate new techniques for application of UHPFRC as strengthening material with the optimum result and to provide an insight into the key parameters affecting the structural performance of strengthened elements with UHPFRC. Therefore, the present research investigates for the first time the effectiveness of the use of dowels at the interface between UHPFRC and concrete, to improve the connection between these two materials and to eliminate the risk of premature de-bonding. Also, in the present study the effectiveness of the use of three-side UHPFRC jackets has been examined. Both techniques aim to upgrade the structural performance of the existing elements without the use of steel bars in the strengthening layers/jackets. The application of this technique could be easily applied in strengthening applications reducing labouring cost and effort [13-15].

2. Experimental program

2.1 Strengthening techniques

Eight RC beams have been examined in the present research. Two beams were used as control beams without any retrofit, two beams were strengthened with UHPFRC layers without dowels and another two identical beams were strengthened with UHPFRC layers and dowels at the interface. Finally, two beams were strengthened with three-side UHPFRC jackets (Table 1). In all the strengthened beams the surfaces of the initial beams were roughened prior to the casting of the UHPFRC layer.

Table 1 Examined Beams

Beam	Strengthening Technique
P1	Control beam
P2	Control beam
U1	UHPFRC layer
U2	UHPFRC layer
D1	UHPFRC layer and dowels
D2	UHPFRC layer and dowels
3SJ1	UHPFRC Jacket
3SJ2	UHPFRC Jacket

The initial beams (Figure 1) were reinforced using two steel bars grade B500C with 12 mm diameter at the tensile side. Also, shear links of the same steel grade with 10 mm diameter were placed at 150 mm spacing along the length of the beam.

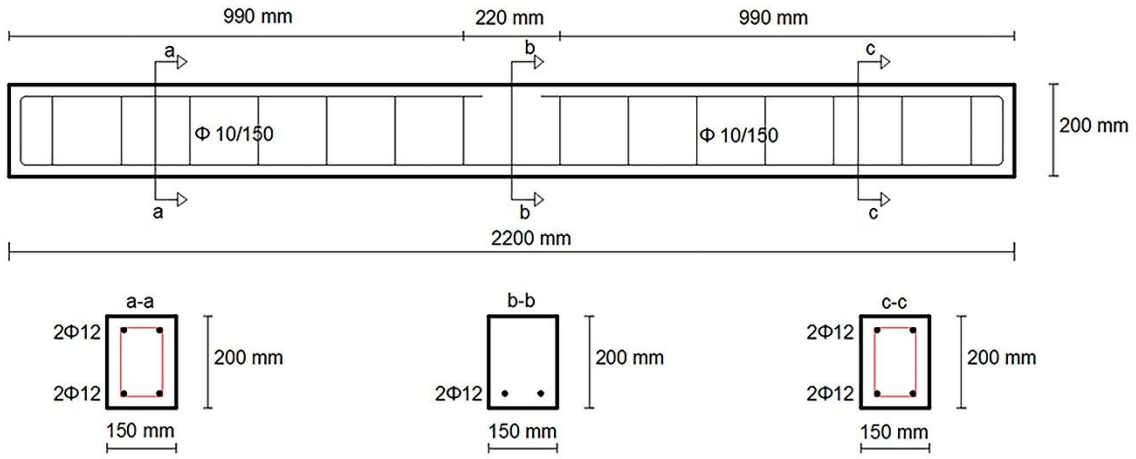

Fig. 1 Geometry and reinforcement of the RC beams

The layers had a depth of 50 mm, a breadth of 150 mm (equal to the breadth of the initial beam) and were cast along the whole length of the tensile side of the beams. As can be seen in Figure 2a, ribbed steel bars with a length of 126 mm, in total, 12 mm diameter and a spacing of 222 mm were used as dowels. The design of dowels was based on the Greek Retrofitting

Code [16]. When steel bars are used as dowels, the minimum required cover in the direction of loading should be at least $5d_b$ for the front cover and $6d_b$ at the back cover (where d_b is the diameter of the bars) to prevent premature failure of the concrete edges around the dowels [16]. On the vertical direction, a cover of at least $3d_b$ is required, while it is also suggested that the length of the bars inside concrete should be at least $8d_b$ [16]. In Figure 2b, the position of the dowels is presented

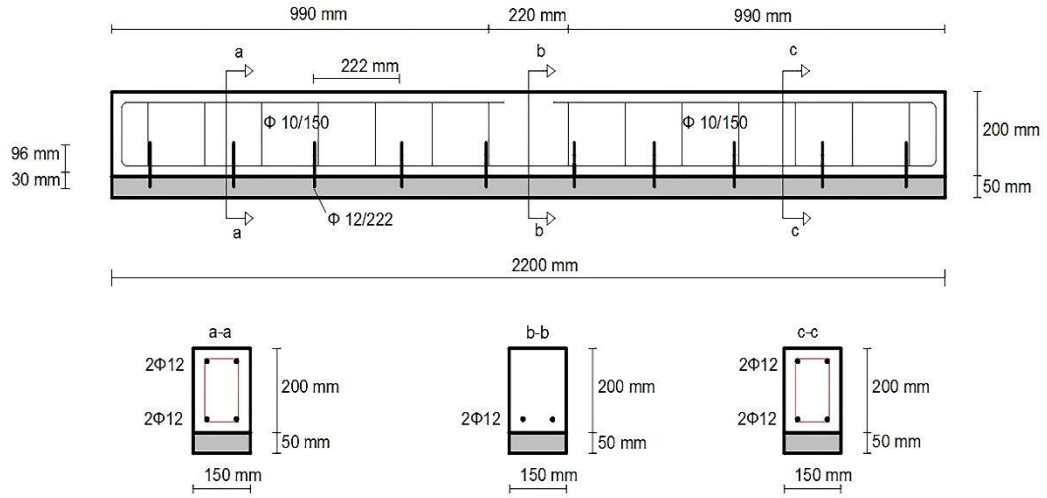

Fig. 2a

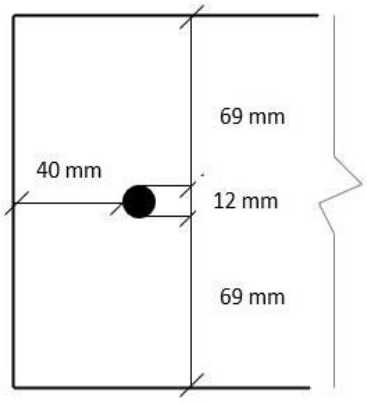

Fig. 2b

Fig. 2 a) Geometry and reinforcement of the strengthened beams with layers and dowels b) Position of the dowels

The strengthening technique and the geometry of the strengthened beams with UHPFRC jackets on three sides is presented in Figure 3.

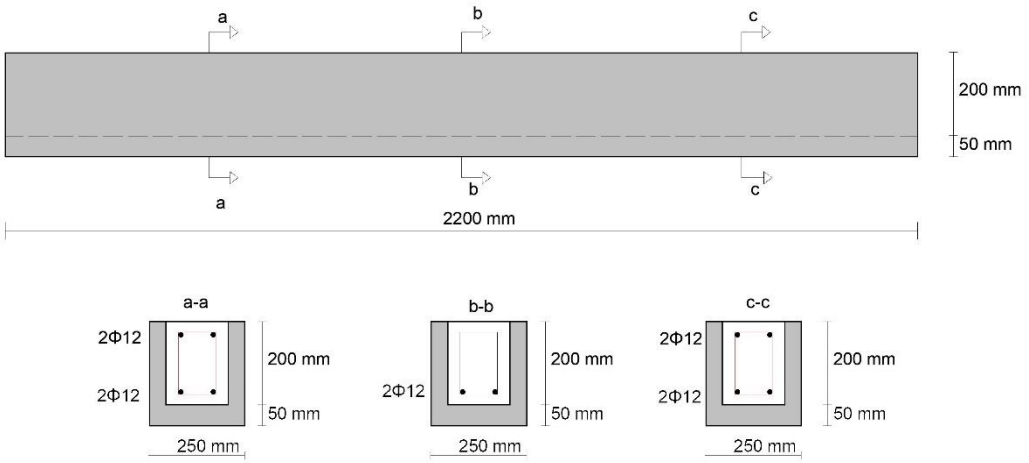

Fig. 3 Strengthening with three-side jackets

As can be seen in Figure 3, a thickness of 50 mm was used for the UHPFRC jacket leading to a beam with total breadth equal to 250 mm and a height of 250 mm. The jackets were cast along the full length of the beams.

2.2 Preparation of the specimens

For the preparation of the UHPFRC, fine sand with a maximum particle size of 500 μm was used together with microsilica, Ground Granulated Blast Furnace Slag (GGBS) and high strength cement class 52.5 R type I. In addition, steel microfibers with a length of 13 mm and a diameter of 0.16 mm were incorporated in the mix.

According to study [17], a fiber content in the range of 3-4 Vol-%, is considered an optimum content for the preparation of the UHPFRC considering parameters such as; the rheological properties, the performance of the material and the cost. Therefore, in the present study a fiber content of 3 Vol-% was adopted. The mixture design of UHPFRC is presented in Table 2 and the mixture design of the conventional concrete is presented in Table 3.

Table 2 The mixture design for the preparation of UHPFRC

Material	Mix proportions (kg/m^3)
Cement	620
GGBS	434
Silica fume	140
Silica Sand	1051
Superplasticizer	59
Water	185
Steel fibers	235.5 (3 Vol.-%)

Table 3 The mixture design for the preparation of concrete

Material	Mix proportions (kg/m^3)
Cement	340
Fine Aggregates	1071
Coarse Aggregates	714
Water	205

The initial beams were wet cured daily for 28 days. A pistol grip needle scaler was employed and all the strengthened beams were roughened to a depth of 2-2.5 mm. To quantify the surface texture, the sand patch method was used [12]. Once the desired roughening depth was achieved and the surface was ready, the beams were drilled, using an impact drill, and the dowels were placed in position. Based on Technical Specifications on the placement of dowels in concrete elements [18], when steel bars are used as dowels, it is suggested that the diameter of the hole (d_h) should be 4 mm higher than the diameter of the connectors (d_b).

For the connection of the dowels with the beams, a thixotropic structural two-part adhesive was used. According to the specifications from the manufacturer, the compressive strength of the epoxy over 14 days at +15°C was 70-80 MPa, while the tensile strength was in the range of 25-28 MPa.

Before the application of the jackets on the other hand, the beams were roughened on all the three sides. Once the coating was removed and the desired depth was achieved, the beams were cleaned carefully before the casting of the jackets.

The UHPFRC layers and jackets were applied two months after the casting of the initial beams and the strengthened beams were tested after four months. In Figure 4, the procedure for the preparation of the strengthened beams with layers and dowels (Figure 4a and 4b) and jackets (Figure 4c) is presented.

Fig. 4a **Fig. 4b** **Fig.4c**

Fig. 4 a) Drilling of the initial RC beam b) dowels in place c) roughened beam on 3 sides

2.3 Properties of the materials

Three cubes of 100 mm side were tested to identify the compressive strength of both conventional concrete and the UHPFRC. The compressive tests were conducted following the BS EN 12390-3:2009 [19]. The samples were obtained from the same batch with the examined specimens, water cured at ambient temperature for 28 days and tested the same day with the testing of the beams. The average compressive strength of the conventional concrete cubes was

30.9 MPa and the standard deviation was found to be equal to 2.34 MPa. The average compressive strength of the UHPFRC on the other hand, was found to be equal to 136.5 MPa and the standard deviation was 5.5 MPa.

The tensile properties of the UHPFRC were evaluated using six dog-bone shaped specimens (Figures 5a-b). Tests were conducted under constant loading with a displacement rate of 0.007 mm/sec, which is the same loading rate has been used in other studies [3,4,12] leading to comparable results. The tensile stress-strain results are illustrated in Figure 5c. From the average curve, the maximum stress was found to be equal to 11.5 MPa, the elastic limit was 5 MPa and the modulus of elasticity was calculated equal to 51 GPa. All the specimens were tested the same day with the strengthened beams.

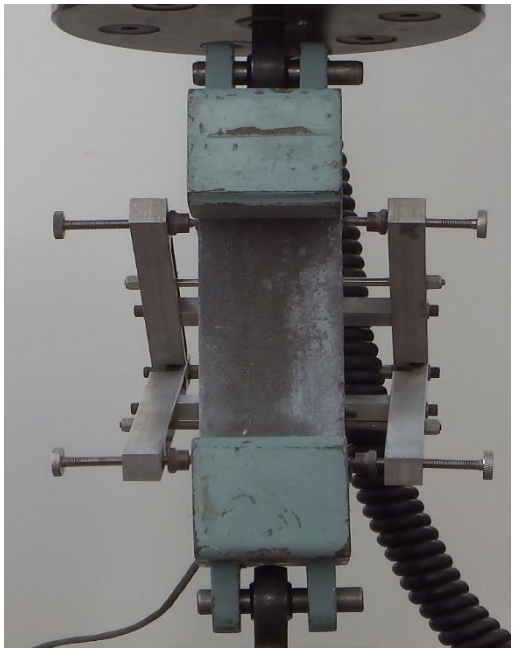

Fig. 5a

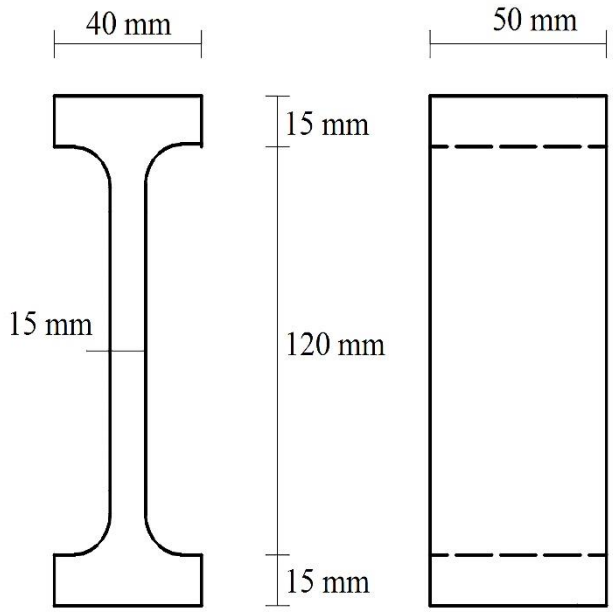

205

206 **Fig. 5b**

207

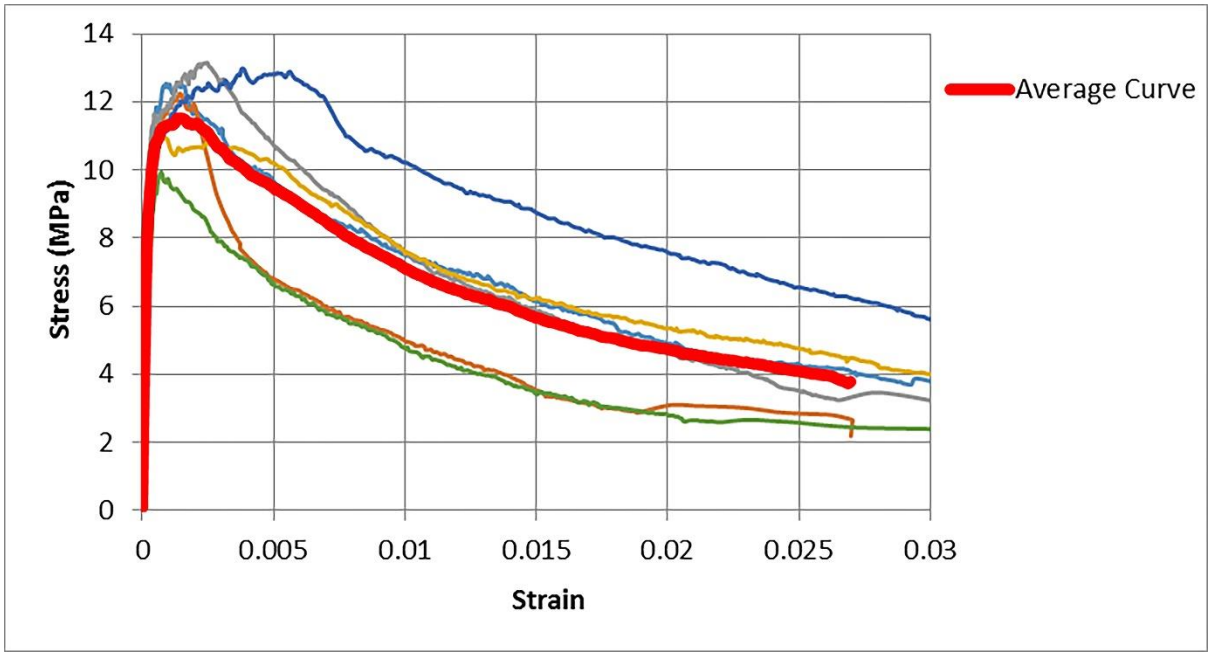

208

209 **Fig. 5c**

210 **Fig. 5** a) Dog bone specimen before Testing b) Dimensions of the Dog bone Specimen c)

211 Experimental results from the direct tensile tests of UHPFRC

2.4 Testing of the beams

The examined beams, were tested under a four-point loading test with a displacement rate of 0.008 mm/sec, which is in agreement with the loading rate used by other researchers [12,22] leading to comparable results The experimental setup for the examined beams is presented in Figures 6 a-d.

Fig. 6a

Fig. 6b

Fig.6c

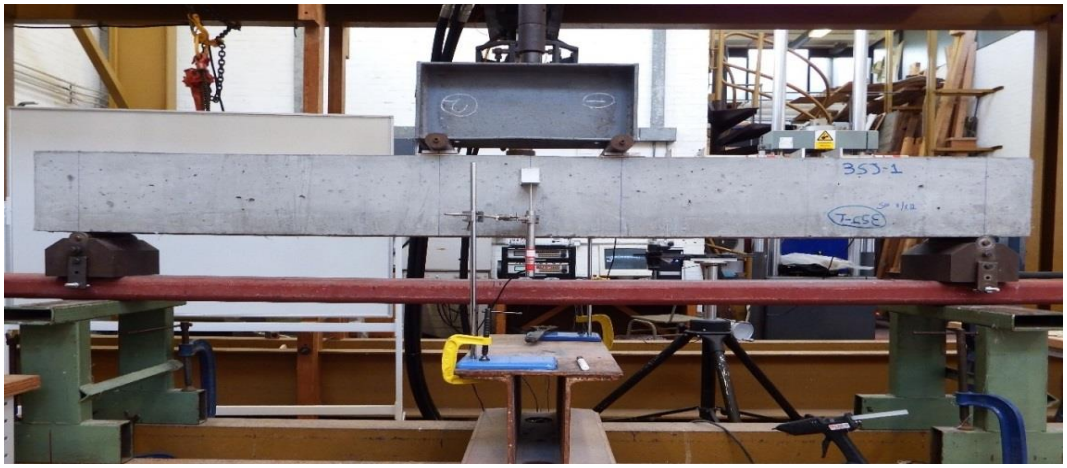

Fig.6d

Fig. 6 Experimental setup for the a) control beam b) strengthened beam with layers c) strengthened beam with layer and dowels d) strengthened beam with jacket

During the testing of the strengthened beams with layers, apart from the load carrying capacity and the deflection, the slips at the interface between UHPFRC and RC were recorded using nine Linear Variable Differential Transformers (LVDTs) in total. As can be seen in Figures 7a and 7b, six LVDTs were placed on side 1 along the full length of the beam, while three LVDTs were placed at the second side to validate the results obtained from side 1.

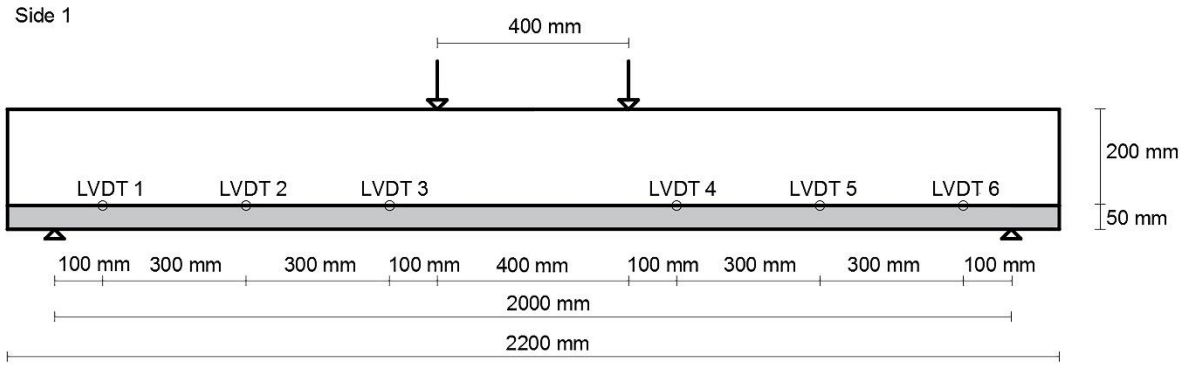

Fig. 7a

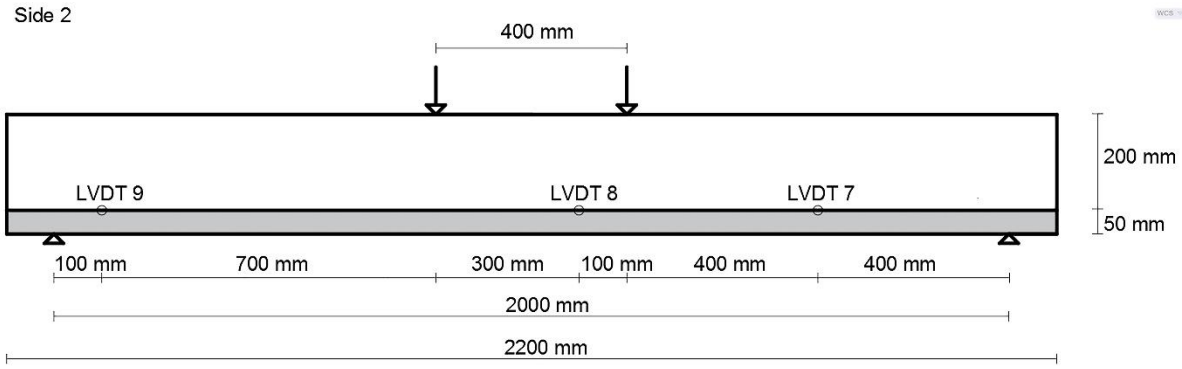

Fig. 7b

Fig. 7 a) Positions of the LVDTs for the measurement of slips on side 1 b) positions of the LVDTs for the measurement of slips on side 2

2.5 Experimental results of the examined beams and discussion

The experimental results for the control beams, the strengthened beams with UHPFRC layers, the strengthened beams with UHPFRC layers and dowels and the strengthened beams with jackets are presented in Figure 8.

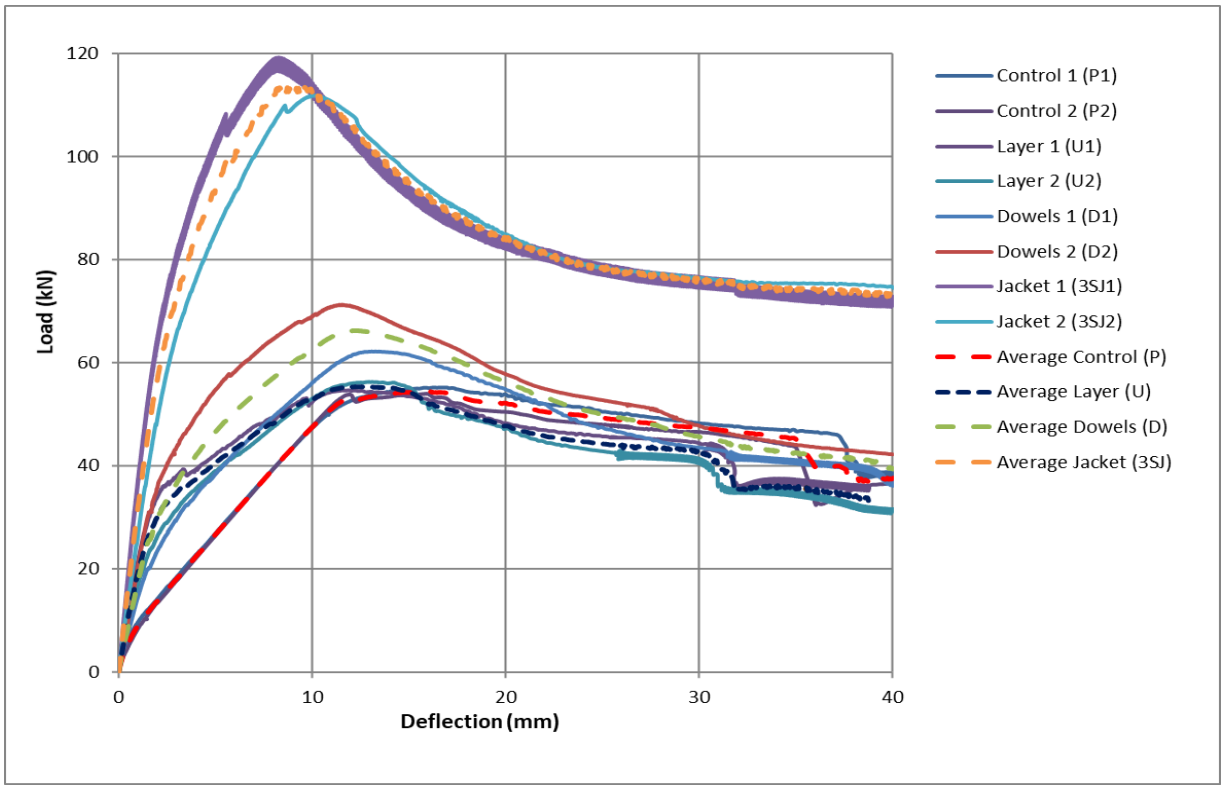

Fig. 8 Experimental results for all the examined beams

246 The average load-deflection results, for all the examined beams, are presented in the same
247 graph in Figure 9.

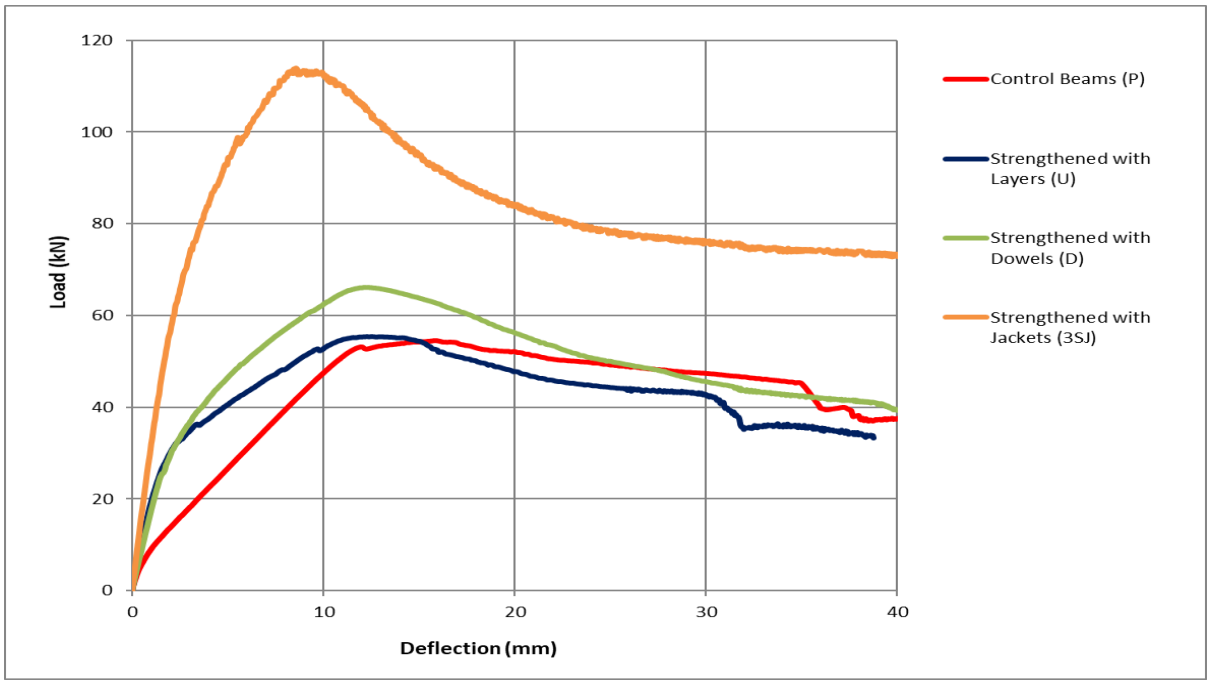

248

249 **Fig. 9** Average load-deflection results

250 From Figure 9, the end of the linear part for each configuration was identified and is
251 representing the formation of significant cracks, and the values are presented in Table 4. In this
252 table, the average values for the maximum load, the stiffness and the displacement at the
253 maximum load are also presented.

254 **Table 4** Maximum load and Stiffness for all the examined beams

Beam	Maximum load (kN)	Stiffness (kN/mm)	Start of Cracking (kN)	Displacement At Peak Load (mm)
Average P1,2	54.6	9.2	5	15.8
Average U1,2	55.3	21.5	15	12.3
Average D1,2	66.2	18.3	24	12
Average 3SJ 1,2	114.5	34	58	8.6

255

The results of Figure 8, show a small scatter of the results of the identical samples. As illustrated in this figure, similar values were achieved for the maximum load of beams P1 and P2 (55.1 kN for beam P1 versus 54 kN for beam P2) and the stiffness (10.5 kN/mm for beam P1 versus 8.4 kN/mm for beam P2). Considering the average load-defection curve, the maximum load was found to be equal to 54.6 kN, the stiffness was calculated to be 9.2 kN/mm and the deflection at the maximum load was equal to 15.8 mm.

The load-deflection results obtained for the identical beams U1 and U2 are also presented in the same graph in Figure 8. From this figure, it is clear that there is a positive agreement in the experimental results for both the identical beams in terms of maximum load (54.6 kN for beam U1 versus 56.3 kN for beam U2) and the stiffness (23 kN/mm for beam U1 versus 19.2 kN/mm for beam U2). Based on the average load-deflection curve, the maximum load was found to be equal to 55.3 kN, the stiffness was calculated to be equal to 21.5 kN/mm and the deflection at the maximum load was equal to 12.3 mm.

From Figure 8, it can also be noticed that the load carrying capacity of beam D2 (71.3 kN) and the stiffness (21 kN/mm), were higher compared to the respective values of beam D1 (62.2 kN the maximum load and 16.5 kN/mm the stiffness), which is attributed to imperfections during the preparation of the samples and during the installation of the dowels. However, both beams exhibited higher load carrying capacity compared to beams U1 and U2. Considering the average curve, the maximum load was found to be equal to 66.2 kN, the stiffness was 18.3 kN/mm and the deflection at the maximum load was equal to 12 mm.

From Figures 8 and 9, a big increase in the load the load carrying capacity and the stiffness of the strengthened beams with jackets can be distinguished, compared to all the other techniques. The maximum load of beam 3SJ1 was found to be equal to 119.2 kN and the stiffness was calculated to be equal to 38.8 kN/mm. The maximum load of beam 3SJ2 on the other hand, was found to be equal to 112 kN and the stiffness 30.5 kN. Considering the average

curve, the maximum load was equal to 114.5 kN, the stiffness was 34 kN/mm and the deflection at the maximum load was equal to 8.6 mm.

Considering the average results of Figure 9 and Table 4, it is clear that in all the examined cases the stiffness of the strengthened members was significantly enhanced. Based on the results of the present investigation, the contribution of UHPFRC layers without the use of dowels or any other reinforcement, relies mainly on the delay of the formation of cracks and the significant stiffness enhancement. Based on the average results of Table 4, strengthening with UHPFRC layers resulted in significant stiffness increment (134%), while the load capacity was only slightly increased by 1.5% . These results are also in agreement with other studies in the literature review [10,12]. In these studies it was highlighted that the main contribution of UHPFRC layers is on the delay of the formation of cracks and the significant increment of the stiffness. On the contrary, the contribution UHPFRC layers in the load carrying capacity is lower.

From Figure 9 and Table 4, it can also be observed that the addition of dowels, apart from the increment of stiffness, resulted in a significant enhancement of the load bearing capacity of the strengthened beams. More specifically, an average increment of 21.5% was identified in this case. On the contrary, the average increment in the load carrying capacity of the strengthened beams U1, U2 was only 1.5%.

During the testing of the strengthened beams with UHPFRC layers and dowels, it was observed that the formation of cracks was delayed compared to the strengthened beams with UHPFRC layers only. This was obvious from the visual inspection of the beams during the testing, and was also reflected to the load-deflection results. From the results of Table 4 it is clear that the addition of dowels at the interface had as a result the delay in the formation of the cracks compared to the strengthened beams without dowels. When dowels were placed at

the interface between RC and UHPFRC, cracking was initiated at a load value 60% higher compared to the beams with UHPFRC layers without dowels.

The results of the present investigation also indicate that the construction of jackets on three sides is also a very effective strengthening technique which can improve the performance of the strengthened members. From Figure 9 and Table 4, it can be seen that the addition of jackets on three side resulted to a remarkable increment of both the stiffness and the load carrying capacity of the strengthened members. In this case, the maximum load was increased by 110% and the stiffness was enhanced by 270%. It can also be seen that the formation of cracks was initiated at a value of load 334% higher compared to the beams strengthened with UHPFRC layer only.

In the literature there are limited applications of jackets for strengthening of RC members. Al-Osta et. [9] investigated different configuration such as strengthening on one side, on two sides and three sides. The biggest load increment (89%) was noticed when three sides jacket was applied. In the present study, the biggest load carrying capacity was also identified for strengthening with UHPFRC jackets, but with a higher increment of 110%.

In comparison with other strengthening techniques in the literature using UHPFRC, the addition of three-side jacket appears to be the most effective in terms of structural performance. Paschalis et al [12], used steel bars in the UHPFRC layers as extra reinforcement for the strengthening of existing RC beams at the tensile side. The geometry of the beams and layers, and the material properties in this study were the same with the present study. The results showed an increment of 89.5% on the maximum load and 111% on the stiffness of the examined beams. These values are lower compared to the jacketed beams, where increment of 110% on maximum load and 334% on the stiffness were achieved.

329 In Figures 10a-f the failure mode of the examined beams is presented.

330

331 **Fig. 10a**

332

333 **Fig. 10b**

334

335 **Fig. 10c**

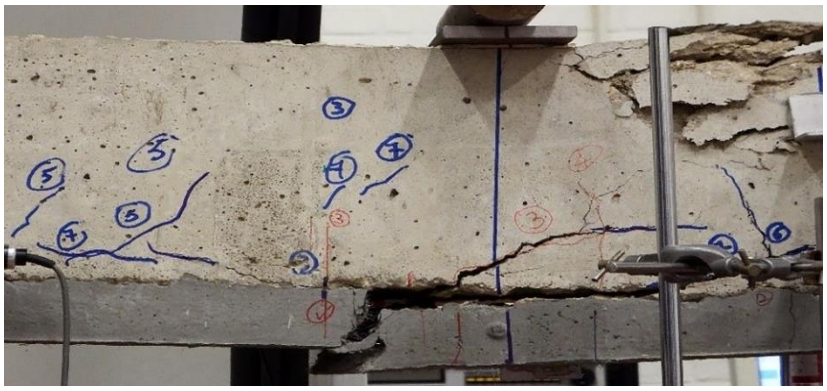

336

337 **Fig. 10d**

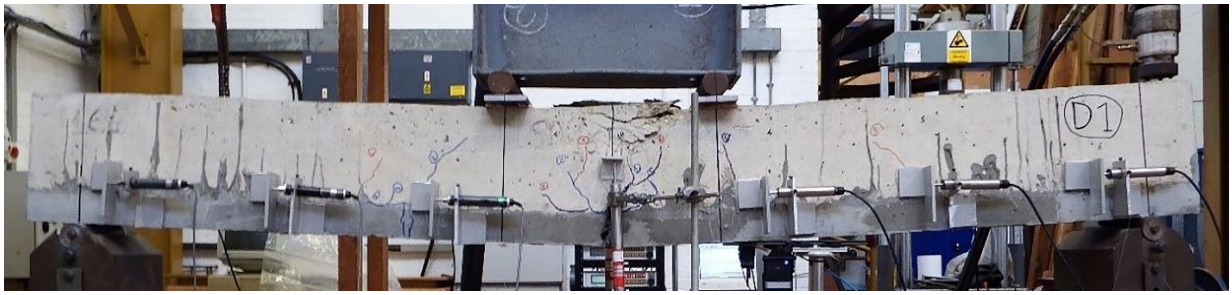

Fig. 10e

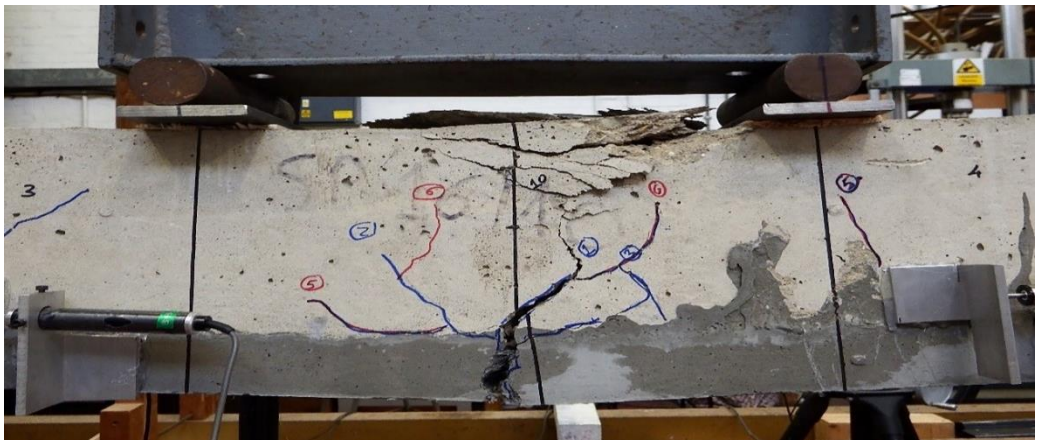

Fig. 10f

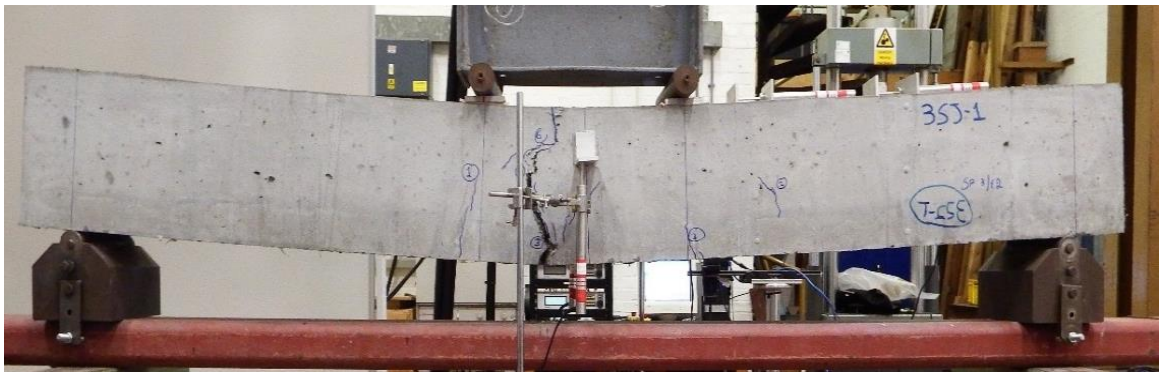

Fig. 10g

Fig. 10 Beams at failure: a) control beam P1 b) strengthened beam with UHPFRC layers U1 c) strengthened beam with UHPFRC layers U2 d) local de-bonding at the interface of beam U1 e) strengthened beam with dowels D1 f) bonding at the interface of beam D1 g) strengthened beam with jacket 3SJ1

The failure mode of the control beams P1 and P2 was identical and was characterized by flexural cracks (Figure 10a). A single crack appeared initially in the middle of the span followed by additional cracks which propagated towards the supports. Inclined shear cracks appeared at a later stage, followed by the crushing of the compressive side at the middle of the span which occurred in the descending branch of the load-deflection curve.

The failure of the beams which were strengthened with UHPFRC layers only, started with a major flexural crack which was initiated at the UHPFRC layers and propagated progressively to the RC beams. Additional minor cracks appeared near the interface during the testing. As can be seen in Figures 10 b-c less cracks appeared in these beams compared to the control beams. However, during of the testing of beam U1, a local de-bonding at the interface between UHPFRC and concrete started when the load reached a value of 48 kN and before the maximum load carrying capacity (Figure 10d). After post-testing inspection of the specimen, it was observed that parts of the interface of this specimen had lower roughness depth, therefore the premature failure of this specimen is attributed to the insufficient interface treatment. On the contrary, the bonding at the interface of beam U2 was effective (Figure 10c), and in this case de-bonding was prevented and typical flexural failure occurred at the middle of the span length, followed by crushing of the compressive side.

The failure mode of beams D1 and D2 was identical. The dowels resulted in a strong bonding between UHPFRC and concrete and de-bonding was prevented in both cases. The specimens failed with a single flexural crack in the middle of the span. These cracks appeared on the UHPFRC layer and progressively propagated to the RC beam resulted in the failure of the beams. Additional minor inclined cracks appeared during the testing of the beams (Figure 10e). Crushing of the compressive side occurred at the post peak load-deflection region. In Figure 10f it can be seen that one single crack started from the layer and propagated at exactly the same position of the RC beam. This shows very good connection at the UHPFRC-to-

374 concrete interface which is attributed to the addition of dowels. The enhancement of the
375 interface connection and the prevention of de-bonding which was achieved in this case shows
376 the beneficial contribution of the dowels. This needs to be considered in real life strengthening
377 applications where interface treatment imperfections may exist and this may lead to de-bonding
378 and failure of the elements as occurred in specimen U1.

379 Beams 3SJ1 and 3SJ2 which were strengthened with jacket on three sides, failed in a
380 similar way with a main flexural crack at the tensile side. As can be seen in Figure 10g, the
381 position of the major crack of beam 3SJ1 was in the middle of the span length. Beam 3SJ2 on
382 the other hand, failed in the position of close to the loading point. After post testing inspection
383 of this specimen, it was found that at this position the steel fibers were not evenly distributed
384 which may have resulted in failure at this point.

385 To further investigate the crucial topic of the bonding between UHPFRC and concrete,
386 measurements of the slips at the interface in different positions, were also recorded during the
387 testing of the strengthened beams (Figure 7). As aforementioned, a local de-bonding at the
388 interface of beam U1 occurred, and for this reason, the measurements of this beam were
389 ignored. The load versus interface slip results in different positions of beam U2 are presented
390 in Figure 11.

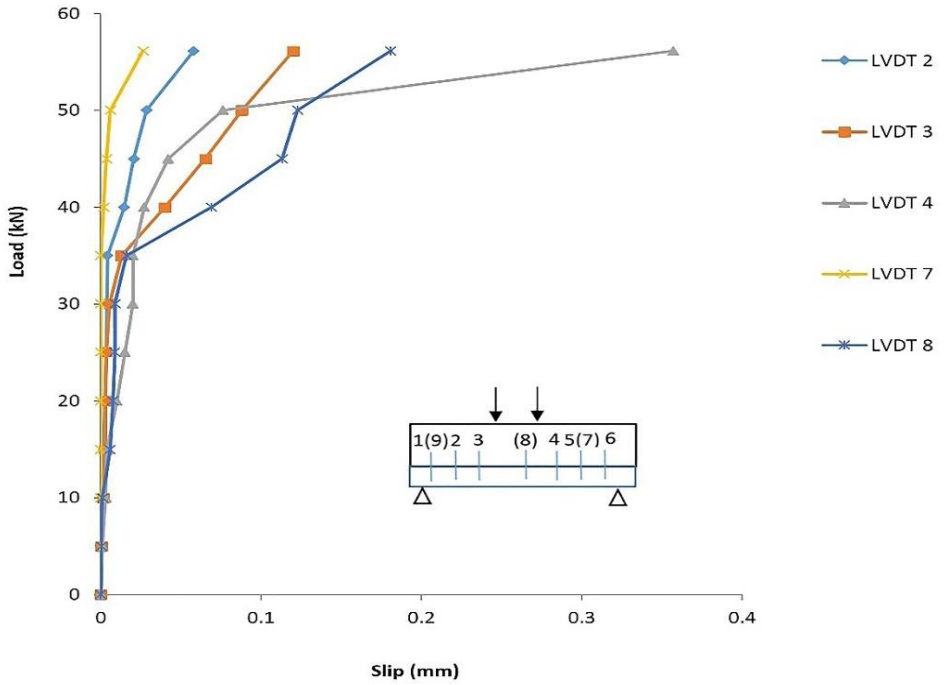

391

392 **Fig. 11** Load versus slip in different positions for beam U2

393 As can be seen in Figure 11, slips were recorded at the positions of the LVDTs 2, 3, 4, 7
394 and 8, while for all the other positions negligible values were recorded indicating good
395 connection (and therefore these points are not included in Figure 11). The maximum value of
396 slip was recorded at the position of LVDT 4 with 0.36 mm (where the shear is maximum),
397 while a value of 0.18 mm was recorded at the position of LVDT 8, which is located between
398 the two loading points. Values in the range of 0.03-0.12 mm were recorded at the positions of
399 LVDTs 2, 3 and 7. Zero values were recorded at the positions close to supports, as expected,
400 due to the high shear strength at these points resulting from the support reactions.

401 The measurements of the slips at the interfaces of beams D1 and D2 are presented in
402 Figures 12a and 12b.

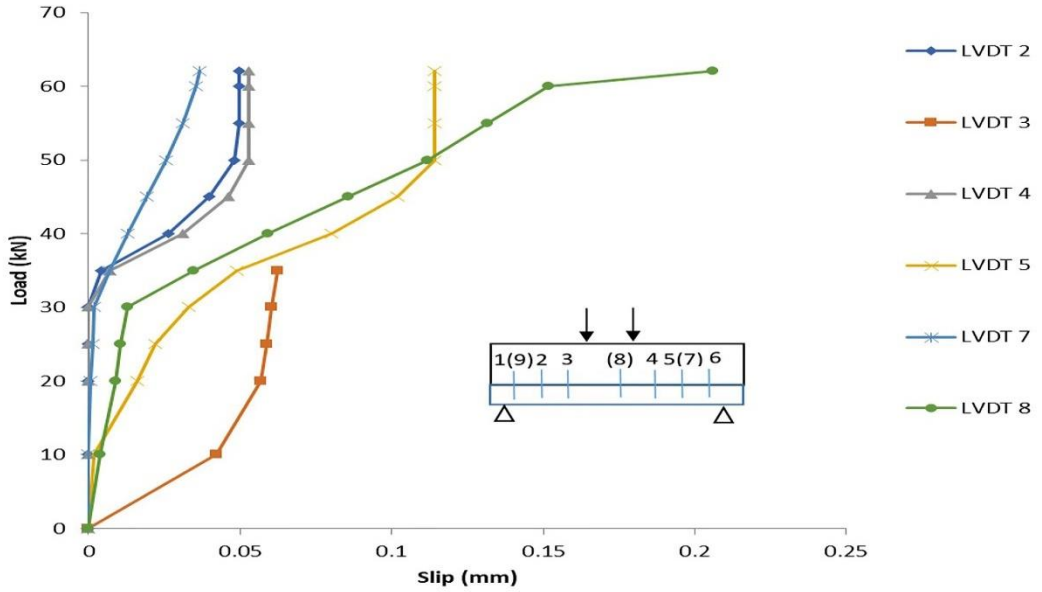

403

404 **Fig. 12a**

405

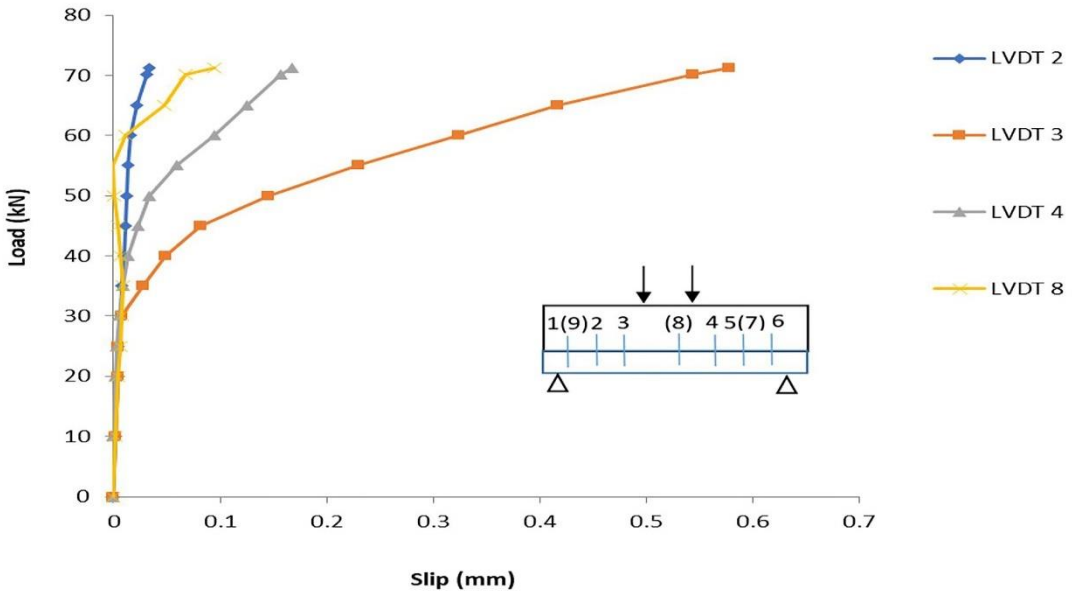

406

407 **Fig. 12b**

408 **Fig. 12** a) Load versus slip in different positions for beam D1 b) load versus slip in different
409 positions for beam D2

410 As shown in Figure 12a, the maximum value of slip of beam D1 was recorded at the
411 position of LVDT 8, located between the two loading points, while only negligible slip values
412 were recorded at the area close to the supports (and these points are not presented in Figure

12a). By contrast, values between 0.036 mm and 0.055 mm were recorded at the positions of LVDTs 2, 4 and 7. Due to the fact that the metal angle section which supported LVDT 3 was detached from the beam at a load value of 35 kN, these measurements are missing.

The measurements of slips at the interface of beam D2 are presented in Figure 12b. As can be seen, slips were recorded only at the positions of LVDTs 2,3,4 and 8. Small values of 0.033 mm and 0.088 mm were recorded at positions 2 and 8 respectively. The highest values of slip were recorded at the positions 3 and 4. It is worth mentioning that the failure of the beam occurred in the area near the position of LVDT 3, leading to higher readings at this point.

A comparison between the recorded values of slip of beams U2, D1, D2 for a load value equal to the maximum load of beam U2 (56.3 kN) is presented in Table 5.

Table 5 Slip measurement for the beams U2, D1, D2 for value of load 56.3 kN

Position	Beam U2	Beam D1	Beam D2
LVDT 2	0.06	0.04	0.01
LVDT 3	0.11	0.01	0.19
LVDT 4	0.357	0.05	0.06
LVDT 7	0.03	0.03	0
LVDT 8	0.18	0.14	0.01

The result of Table 5 indicate that the recorded values of slip at beams D1 and D2 were significantly lower compared to the respective values of beam U2 in almost all the examined positions. Based on these results, it can be seen that only the recordings of LVDT 3 of beam D2 were slightly higher than the respective values of U2 beam, which is attributed to the local failure of the beam at this point.

Existing codes [20, 21] set limit values for different performance levels. The Greek Code of Interventions [20], proposes a maximum slip value of 0.2 mm for the immediate

occupancy performance level, 0.8 mm for the life safety performance level and 1.5 mm and the collapse prevention performance level. All the recorded values in the present study are lower than 0.8 mm, which corresponds to the life safety prevention level. It is worth noticing that most recorded values of the strengthened beams with dowels, are lower than 0.2 mm and only in the position of LVDT3 of beam D2, which was affected by the failure of the beam in this area, a higher value was recorded. According to the fib Bulletin 43 [21] on the other hand, a maximum interface slip of 0.2 mm is suggested for the serviceability limit state and 2.0 mm for the ultimate limit state.

In the literature there are recorded slip values for concrete to concrete interfaces in case of beams strengthened with conventional concrete layers. Tsioulou et al [22], reported a maximum value of slip of 1.1 mm for conventional concrete to concrete interfaces. In this study, RC beams strengthened with RC layers without the use of dowels at the interface. This value is significantly higher compared to the recorded values of the present investigation for UHPFRC to concrete interfaces and according to Greek retrofitting code corresponds to collapse prevention performance level.

The results of the present experimental investigation indicate that the use of dowels at the interface is an effective technique which should be taken into consideration when UHPFRC layers are used for the structural upgrade of existing RC structures. The use of dowels delay the formation of the cracks and result to lower slip values and higher load carrying capacity.

3. Numerical modelling of the examined technique

3. 1 Modelling of the technique

To further investigate the crucial topic of the effect of the interface conditions on the performance of the strengthened elements a numerical investigation has been conducted. Concrete was modelled with an eight-node element using the SBETA constitutive model [23].

In Figure 13, the model used to simulate the behaviour of concrete in tension and compression, is presented.

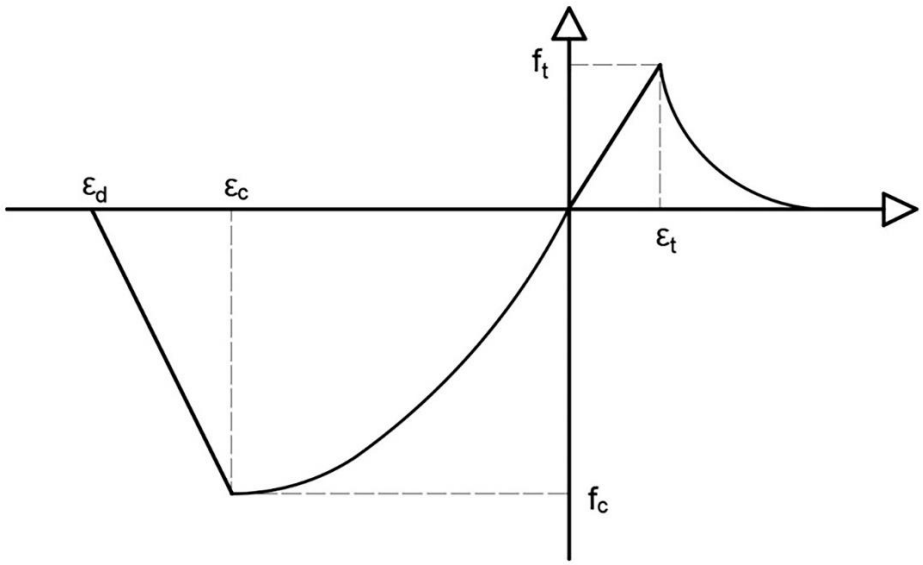

Fig.13 Constitutive model in tension and compression adopted in ATENA software

The steel bars were simulated using linear elements with bi-linear behavior and hardening, as presented in Figure 14. The properties of steel grade B 500C, according to BS 4449:2005 [24] were adopted for the modelling of the steel bars, while the cover of the steel bars was the same as the experimental investigation.

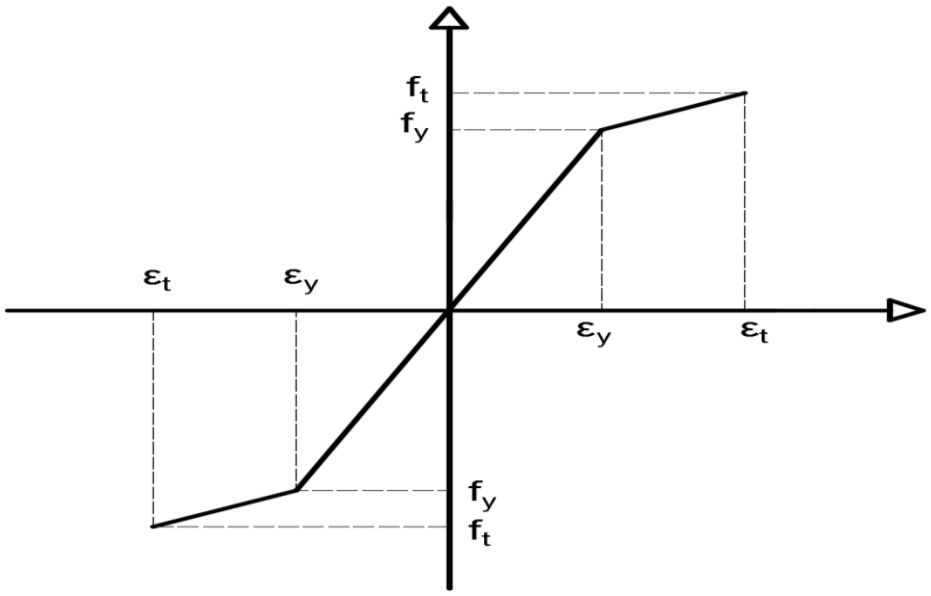

Fig. 14 Stress-strain model of the reinforcement

The concrete to steel bars bond was also taken into consideration. More specifically, the CEB-FIB model code 90 [25] bond-slip model was adopted for the numerical modelling.

The interface between UHPFRC and concrete was modelled using two dimensional contact elements with a coefficient of friction equal to 1 and cohesion 1.8 MPa, which were determined using experimental data from a previously published study [12]. For the numerical modelling of the strengthened beams with dowels, perfect connection at the interface was considered.

For the modelling of the UHPFRC, the compressive and tensile characteristics obtained experimentally were adopted. In compression, SBETA constitutive model [23] was used, while for the modelling of the performance of the material in tension, the average stress-strain results of Figure 5b were used. Based on these results, the response of the material in tension was considered linear up to a value of stress level equal to 5 MPa, while a second part, up to the maximum point, was used to model the strain hardening. After the ultimate stress, there is the strain softening phase which was modelled with a bi-linear model. The model adopted in tension is presented in Figure 15.

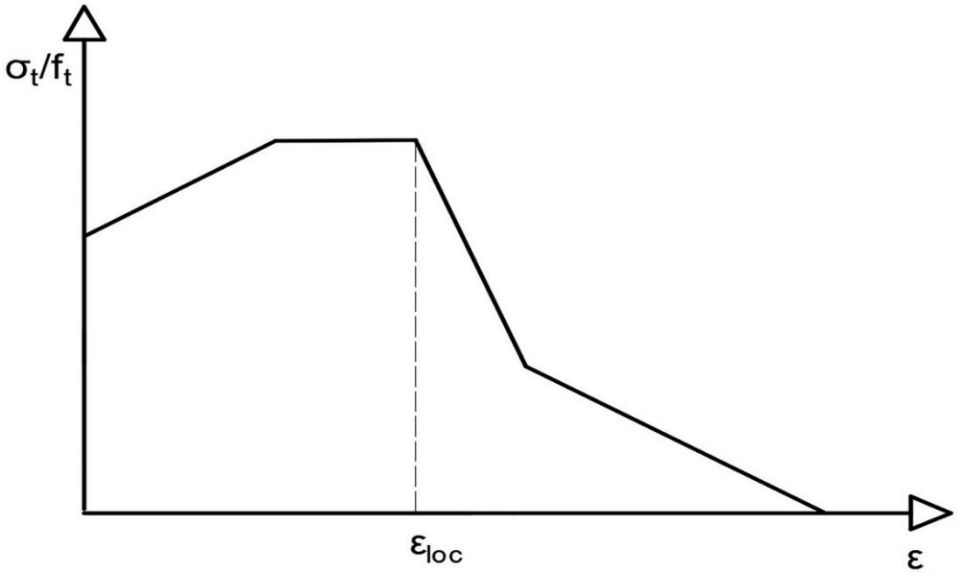

Fig.15 Tensile function adopted in ATENA software for the UHPFRC

For the modelling of the UHPFRC, the shrinkage was also taken into consideration using a negative volumetric strain value to the UHPFRC elements. Based on existing study in the literature review [3], an ultimate value of shrinkage equal to 565 microstrain was recorded for a fiber content of 3% and this value applied to the UHPFRC layers.

3.2 Validation of the numerical model

A comparison between the average experimental and numerical results of the control beam (P), the strengthened beams with UHPFRC layers without dowels (U), the strengthened beams with dowels (D) and the strengthened beams with jackets ((3SJ) are presented in Figures 16a-d respectively.

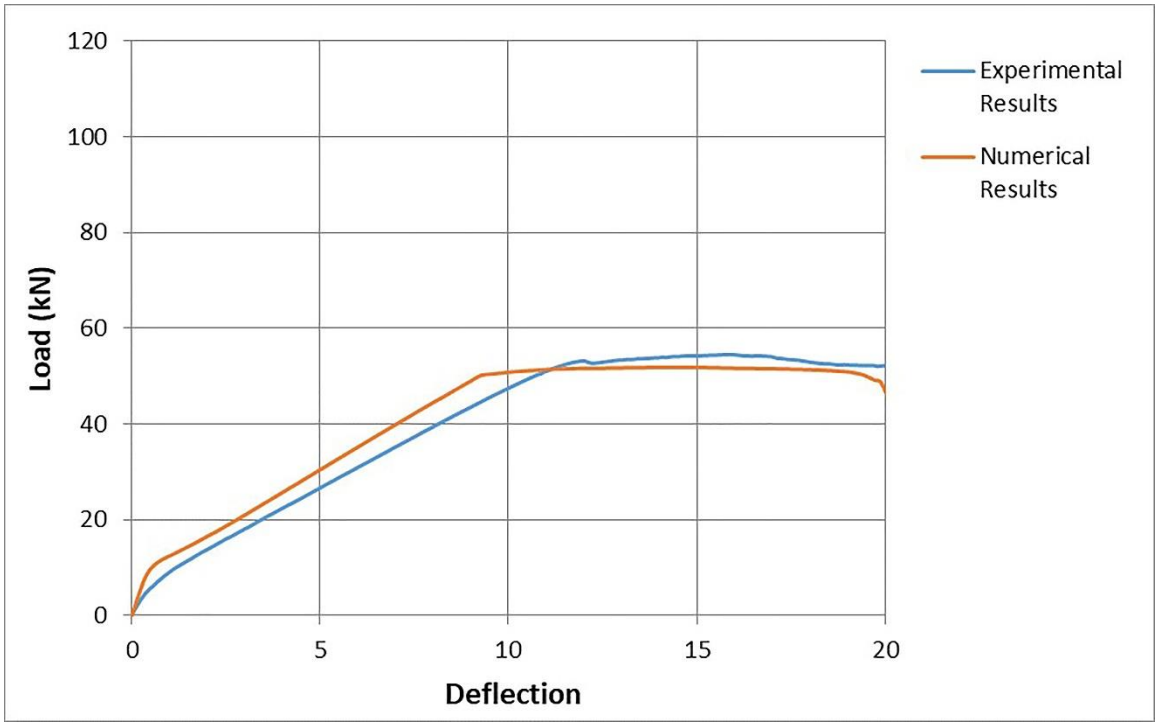

Fig.16a

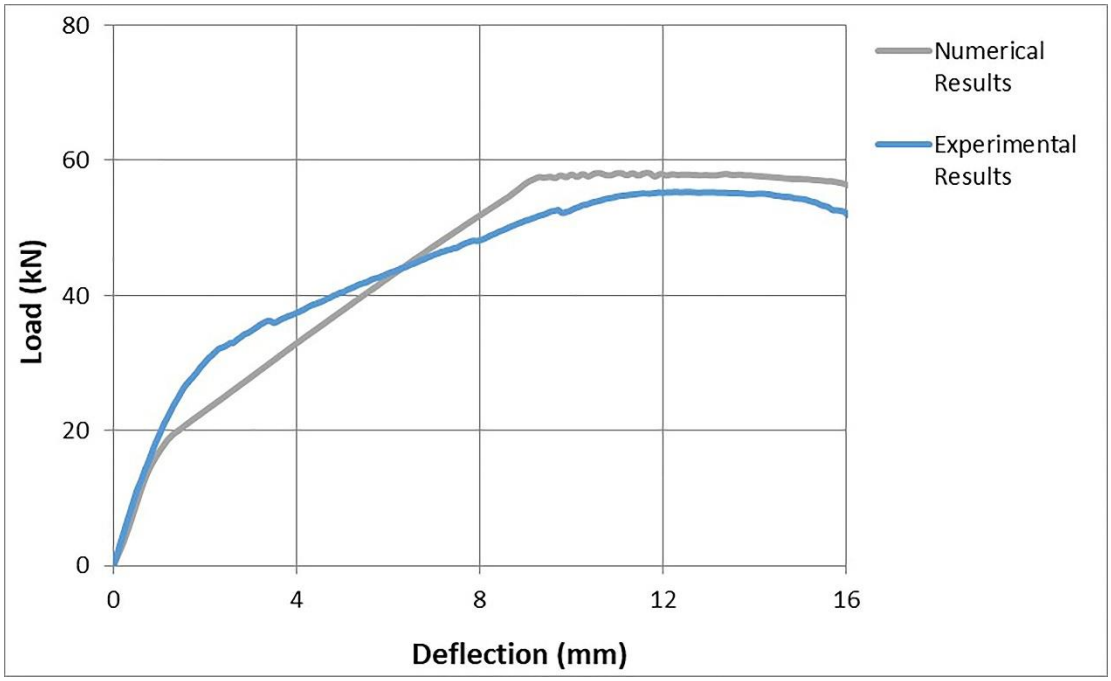

494

495 **Fig.16b**

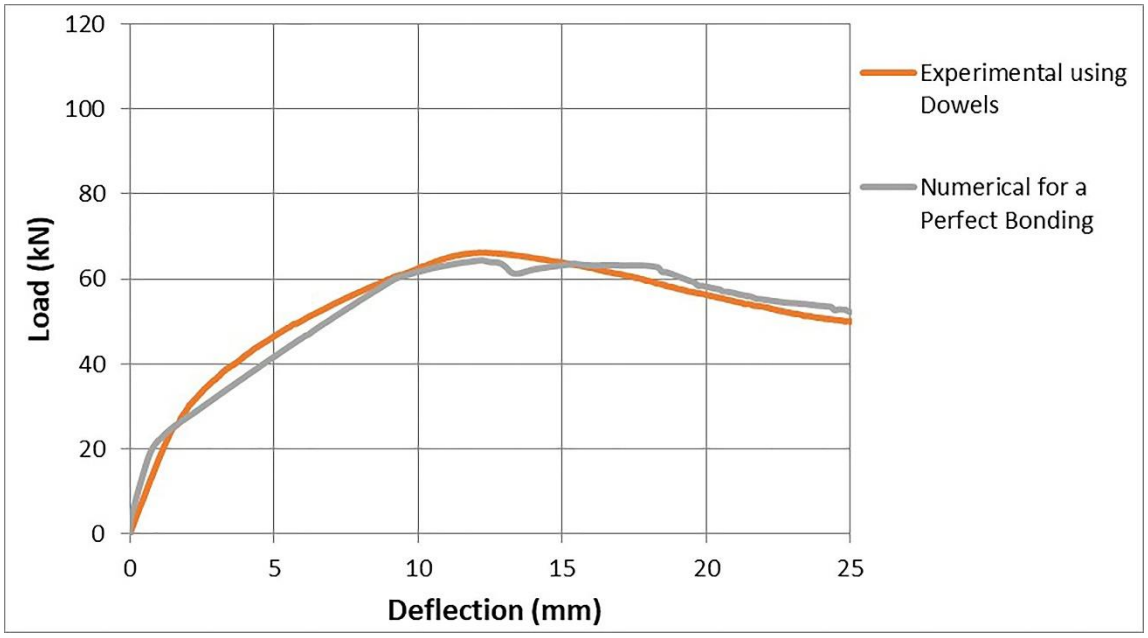

496

497 **Fig.16c**

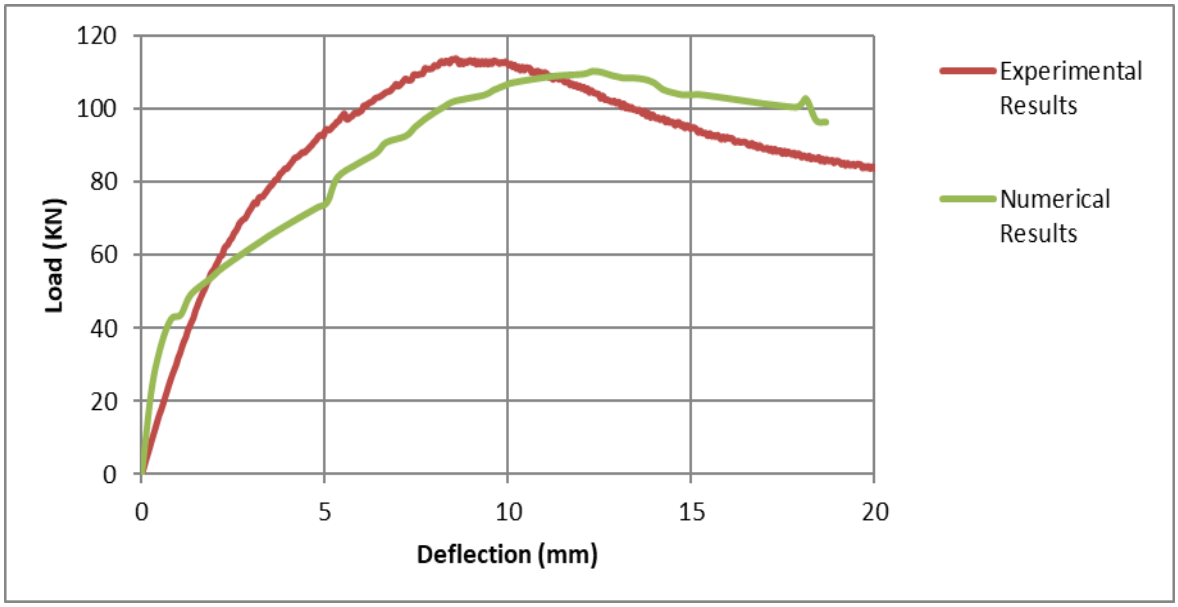

498

499 **Fig.16d**

500 **Fig. 16** Experimental versus numerical results for a) the control beam P b) the beam
501 strengthened with layers U c) the beams strengthened with beams and dowels D d) the beams
502 strengthened with jackets

503 The results of Fig. 16a indicate that there is a very good agreement between the
504 experimental and the numerical results for the control beams. For the strengthened beams with
505 layers (Fig. 16b), the use of contact elements with coefficient of friction equal to 1 and cohesion
506 equal to 1.8 MPa leads to numerical results very close to the experimental. In case of the
507 strengthened specimens with dowels (Fig. 16c), the assumption of perfect bonding at the
508 interface of the beam of the numerical model shows a remarkable agreement with the beam of
509 the experimental investigation with the addition of dowels. Finally, a good agreement between
510 the experimental and the numerical results can be observed for the beams strengthened with
511 jackets. The load carrying capacity of the numerical model (110 kN) is very close to the
512 respective experimental value (114.5 kN), while slightly higher stiffness is obtained
513 numerically.

514 The failure mode of the examined numerical models at the point where the load capacity
515 has been reduced to 80% of the maximum load, is presented in Figures 17a-c.

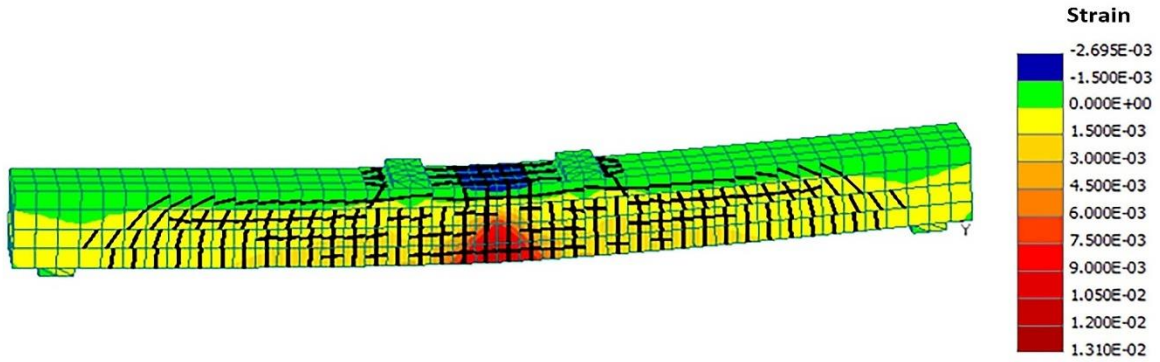

516

517 **Fig.17a**

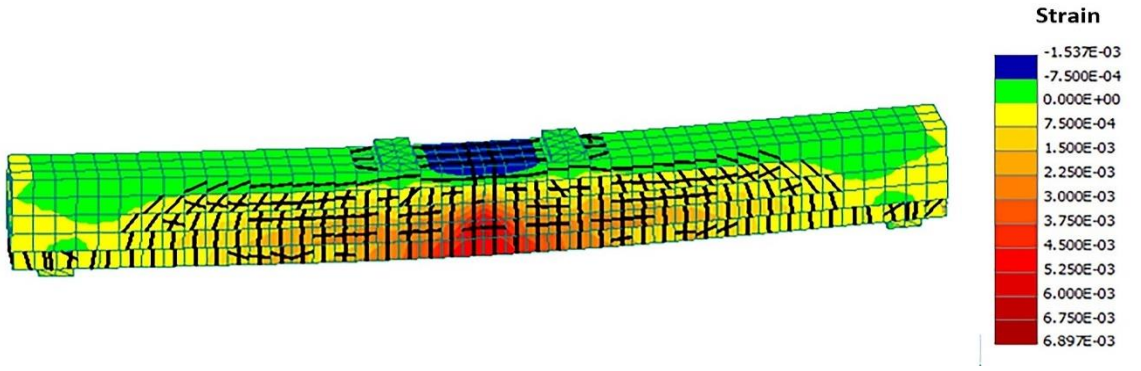

518

519 **Fig.17b**

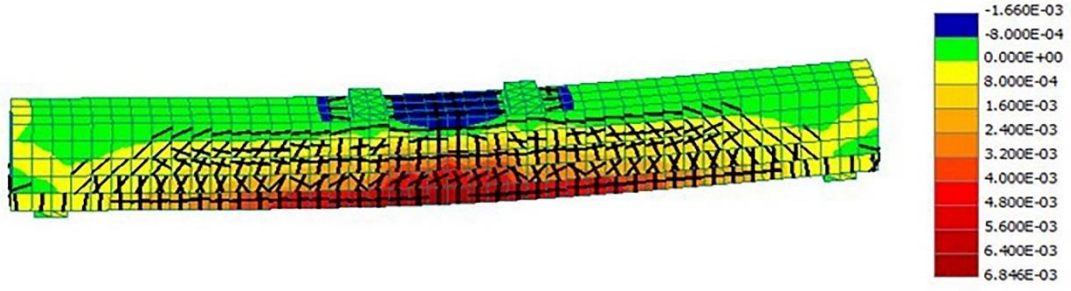

520

521 **Fig.17c**

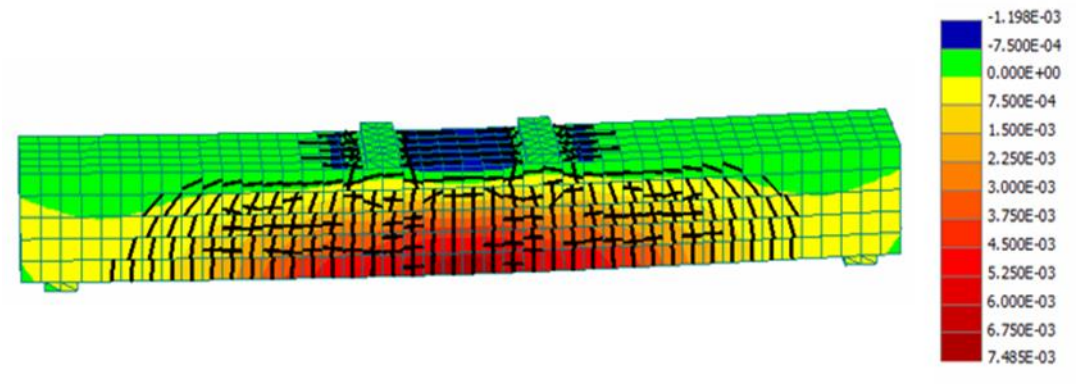

Fig.17d

Fig. 17 Failure mode of a) control beam b) beam strengthened with UHPFRC layer c) beam strengthened with UHPFRC layers and perfect bonding d) beam strengthened with Jacket

The results of Figure 17 indicate that the crack patterns of the numerical models are in a very good agreement with the failure mode observed from the experimental investigation, with high values of strain concentration at the tensile side of the beams and localization of the damage in the middle of the span. Also, in Figures 17a-c high values of strain at the compressive side can be distinguished, similar to the experimental observations where failure at the compressive side occurred (Figures 10a-g).From the experimental results it is evident that the use of dowels results in better bonding between UHPFRC and RC with lower values of slip, while the formation of cracks is delayed. From Figure 16c and the comparison between the numerical results for monolithic connection and the experimental results using dowels, it is clear that when dowels are used, the response of the strengthened beams approaches the respective monolithic of the beam of the numerical investigation, as assumed for the application of the model. In addition, as can be seen in Figure 17c, for a monolithic connection, the strain is distributed along the whole length of the beam and is not concentrated on a small area of the examined specimens. This allows the material of the layer (UHPFRC) to be better utilized and the crack localization to be delayed leading to higher load capacity and enhanced

structural performance, highlighting the beneficial effect of the use of dowels at the UHPFRC-to-concrete interfaces.

4. Conclusions

The present research focused on the investigation of new techniques for the application of UHPFRC as strengthening material without the use of additional steel bars in the strengthening layers, aiming to offer improved structural performance. The first examined technique focused on the investigation of the effectiveness of dowels at the interface between UHPFRC and concrete for the strengthening of RC beams and the second technique investigated the performance of strengthened beams using three-side UHPFRC jackets.

Extensive systematic experimental work has been conducted followed by a numerical study focused on the effect of the interface conditions. The following conclusions can be drawn:

- The contribution of UHPFRC layer (without dowels) can be efficient for the serviceability limit state. The experimental results of the present study recorded high values of slip after this state, which can lead to debonding and lower load carrying capacity.
- Dowels at the interface between UHPFRC and RC result in better bonding, with lower interface slip values preventing de-bonding. Also, dowels delay the formation of cracks.
- The addition of dowels at the interface leads to enhanced load carrying capacity of the strengthened beams. The experimental results of the present study indicated an increase of 21.5% of the load carrying capacity when dowels were used at the interface. The respective increase without the use of dowels was only 1.5%.
- The addition of dowels at the interface leads to better distribution of the stresses along the length of the strengthened elements.

- Superior performance between the examined techniques was achieved for strengthening with three-side jackets. In this case, the load carrying capacity was increase by 110% and the stiffness by 270%.
- A remarkable agreement was identified from the comparison of the experimental results using dowels with the numerical results considering monolithic connection at the interface between UHPFRC and RC.

From the results of the present study it is clear that both, the addition of dowels and jackets, are effective techniques which can improve the performance of the strengthened elements. The selection of the appropriate technique should be depended on the desired outcome of the technique to increase the strength, the stiffness or both.

The use of dowels is a technique which should be taken into consideration to reduce the effect of imperfections during the roughening of the interface and to eliminate the risk of premature de-bonding of the strengthening layer. The construction of jackets on the other hand, should be preferred in heavily damaged RC members or in cases where the load carrying capacity and stiffness need to be significantly increased.

Acknowledgements

The authors would like to acknowledge Sika Limited and Hanson Heidelberg Cement Group for providing raw materials.

REFERENCES

[1] Ferrara, L., Ozyurt, N., Di Prisco, M., “High mechanical performance of fibre reinforced cementitious composites: the role of "casting-flow induced" fibre orientation”, Materials and Structures, 2011, 44 (1), 109-128.

586 [2] Nicolaides, D., Kanellopoulos, A., Petrou, M., Savva P., Mina A., “Development of a new
587 Ultra High Performance Fibre Reinforced Cementitious Composite (UHPFRCC) for impact
588 and blast protection of structures”, Construction and Building Materials, 2015, 95, 667-674

589 [3] Paschalis, S.A., Lampropoulos, A., “Fiber content and curing time effect on the tensile
590 characteristics of Ultra High Performance Fiber Reinforced Concrete (UHPFRC)”, Structural
591 Concrete, 2017, 18 , 577-588

592 [4] Paschalis, S.A., Lampropoulos A., “Ultra High Performance Fiber Reinforced Concrete
593 Under Cyclic Loading”, ACI Materials Journal, 2016, 113 (4), 419-427

594 [5] Kang, S.T., Kim, J.K., “The relation between fiber orientation and tensile behavior in an
595 Ultra High Performance Fiber Reinforced Cementitious Composites (UHPFRCC)”, Cement
596 and Concrete Research, 2011, 41(10), 1001-1014

597 [6] Tsioulou, O., Lampropoulos, A., Paschalis, S.A., “Combined Non-Destructive Testing
598 (NDT) method for the evaluation of the mechanical characteristics of Ultra High Performance
599 Fibre Reinforced Concrete (UHPFRC)”, Construction and Building Materials, 2017, 131, 66-
600 77.

601 [7] Vaitkevicious V., Serelis E., Vaiciukyniene, Raudonis V.,Rudzionis Z., “Advanced
602 mechanical properties and frost damage resistance of ultra-high performance fibre reinforced
603 concrete”, Construction and Building Materials, 2016, 126, 26-31

604 [8] Bruhwiler, E., Denarie E., “Rehabilitation of concrete structures using Ultra-High
605 Performance Fibre Reinforced Concrete”, The Second International Symposium on Ultra High
606 Performance, 2008, Kassel, Germany

607 [9] Al-Osta, M., Isa, M., Baluch, M. & Rahman, M., 2017. Flexural behaviour of reinforced
608 concrete beams strengthened with ultra-high performance fiber reinforced concrete.
609 Construction and Building Materials, Volume 134, pp. 279-296.

610 [10] Safdar M., Takashi Matsumoto T., Kakuma K, Flexural behavior of reinforced concrete
611 beams repaired with Ultra High Performance Fiber Reinforced Concrete (UHPFRC),
612 Composite Structures, 2016, 157, 448-460.

613 [11] Lampropoulos, A., Paschalis, S.A., Tsioulou O., Dritsos S., "Strengthening of reinforced
614 concrete beams using ultra high performance fibers reinforced concrete (UHPFRC)",
615 Engineering Structures, 2015, 106, 370-384.

616 [12] Paschalis, S.A., Lampropoulos, A., Tsioulou, O., "Experimental and numerical study of
617 the performance of Ultra High Performance Fiber Reinforced Concrete–Reinforced Concrete
618 for the flexural strengthening of full scale members", Construction and building materials,
619 2018, 186, 351-366.

620 [13] Trucy l., Dobrusky S., Bonnet E., Ultra-high performance shotcrete: yes we can!,
621 proceedings of UHPFRC 2017 Designing and Building with UHPFRC: New large-scale
622 implementations, recent technical advances, experience and standards, 2017, pp 154 – 163,

623 [14] Ductal, Innovation: Ductal Shotcrete the first sprayed UHPC Accessed on 25-11-2019 at
624 https://www.ductal.com/en/engineering/innovation-ductalr-shotcrete-first-sprayed-uhpc

625 [15] Skazlic M., Skazlic Z. ; and J. Majer J., Application of High Performance Fibre
626 Reinforced Shotcrete for Tunnel Primary Support, 10th International Conference on Shotcrete
627 for Underground Support, Whistler, 2006. p. 206-214.

628 [16] Greek Organization for Seismic Planning and Protection, Greek Retrofitting Code
629 (GRECO), Athens, (in Greek), 2013

630 [17] Paschalis, S.A, Lampropoulos, A., "Mechanical performance and cost correlation of Ultra
631 High Performance Fiber Reinforced Concrete (UHPFRC)", 19th Congress of IABSE
632 Stockholm, 2016, Stockholm, Sweden

633 [18] Hellenic Technical Specification, Placement Dowels in Concrete Elements, Greek
634 Ministry of Environment and Energy, 2009, (In Greek)

635 [19] BS EN 12390-3:2009, Testing hardened concrete-Part 3: Compressive strength of test
636 specimens

637 [20] Greek Retrofitting Code, (GRECO) Greek Organization for Seismic Planning and
638 Protection, Athens, Greek Ministry for Environmental Planning and Public Works, 2013 (in
639 Greek)

640 [21] fib Bulletin No 43, Structural Connections for precast concrete buildings, Lausanne,
641 International Federation for Structural Concrete, 2008

642 [22] Tsioulou, O., Lampropoulos, A., Dritsos, S., Experimental investigation of interface
643 behavior of RC beams strengthened with concrete layers, Construction and Building Materials,
644 40: (2013), 50-59.

645 [23] Cervenka,V., Jendele, L., Cervenka, J., ATENA Program Documentation: Part 1 Theory,
646 Prague, Czech Republic,2013

647 [24] BS 4449:2005 Steel for the reinforcement of concrete. Weldable reinforcing steel. Bar,
648 Coil and Decoiled product. Specification, BSI, (2005)

649 [25] CEB Bulletin No. 213/214, CEB-FIP Model Code 90. International Federation for
650 Structural Concrete, Lausanne, (2013)

651

652